THE ASTROPHYSICAL JOURNAL, 330:51–60, 1988 July 1

INTERACTING BINARY GALAXIES. III. OBSERVATIONS OF NGC 1587/1588 AND NGC 7236/7237

KIRK D. BORNE[1,2,3]
Department of Astronomy, University of Michigan, and Department of Terrestrial Magnetism, Carnegie Institution of Washington
AND
JOHN G. HOESSEL[1,4]
Space Telescope Science Institute[5]
Received 1985 October 3; accepted 1987 December 23

ABSTRACT

The catalog of isolated galaxy pairs prepared by Karachentsev has been culled for its E-E constituents. Major disturbances have been identified in ~10% of all such pairs of ellipticals. CCD pictures and long-slit spectroscopic observations have been obtained at KPNO for the most photometrically distorted of these systems. Such pairs very likely represent strongly interacting, physically associated, binary elliptical galaxies. Radial variations of rotation velocity and velocity dispersion are extracted from the spectroscopic data for each of the two galaxies in a given pair. We describe here such observations for two Karachentsev pairs, Nos. 99 and 564. The observed disturbances in rotation velocity and luminosity distribution are discussed in terms of the gravitational interaction hypothesis. In light of this discussion, we believe that *we have uncovered and identified observational evidence of tidal friction in action.* The evidence includes U-shaped rotation velocity curves and the morphology of the observed luminosity asymmetries. Imaging and dynamical data such as presented here are essential to the numerical simulation of interacting binaries. A preceding companion paper (Paper II) describes a particular physical model and simulation technique, while the following companion paper (Paper IV) presents specific interaction models that successfully match all of the available data for K99 and K564.

In NGC 1587, the brighter component of K99, we find one of the highest rotation rates known for an E2 galaxy of average luminosity. Its rotation rate (in units of the central velocity dispersion) is $v_{rot}/\sigma = 0.6$. Because this rotation is in the same sense as the binary orbital motion, the net angular momentum in this *isolated* binary system is large, challenging simple tidal torque theories to identify the source of this momentum. It is possible that NGC 1587 is itself a merger remnant, with its spin being a relic of the orbital angular momentum in that previous binary interaction.

Subject headings: galaxies: individual (NGC 1587/1588, NGC 7236/7237) — galaxies: internal motions — galaxies: structure

I. INTRODUCTION

Merger scenarios have become quite popular as candidate theories for the formation of various types of galaxies (Toomre 1977; Tremaine 1981; Schweizer 1982, 1983; Borne and Richstone 1982, 1988; Schweizer, Whitmore, and Rubin 1983; Quinn 1984). A large body of theoretical work, which includes quite a number of simulations, has been reported in the literature (see Borne 1984, hereafter Paper I, and references cited therein). Particularly popular have been discussions of mergers among galaxies in rich clusters, with arguments aimed at explaining the formation and observed properties of the supergiant galaxies typically seen in cluster centers (Ostriker and Tremaine 1975; White 1976; Hausman and Ostriker 1978). A growing body of observational evidence which bears on this question is becoming available (e.g., Carter *et al.* 1981; Schneider and Gunn 1982; Schneider, Gunn, and Hoessel 1983*b*; Hoessel and Schneider 1985; Hoessel, Borne, and Schneider 1985; Tonry 1985*b*). As pointed out in Paper I and as discussed in greater detail by others (Tonry 1984, 1985*a*; Merritt 1984; Cowie and Hu 1986), the dynamics of the central regions in rich clusters are not completely understood, and such an environment is clearly not the ideal place to study the physics of galaxy interactions. We believe that studies of isolated interacting pairs will do much to improve our understanding of the dynamical evolution of galaxies.

On another front, a large industry has been devoted over the past 10+ years to the accumulation, through detailed observational work, of fundamental data on the internal dynamics of elliptical galaxies. The observational situation has been reviewed by Illingworth (1981, 1983) and by Davies *et al.* (1983). Considerable effort has been expended on attempts to identify in the present epoch those observable properties of galaxies and of their spheroidal components that yield clues to the formation of these systems. Here again the merger theory is invoked as one of the popular explanations for the origin of some of the properties of spheroidal systems and of massive halos (e.g., White and Rees 1978).

Close pairs of interacting galaxies provide a unique setting for the study of the internal workings of gravitational

[1] Visiting Astronomer, Kitt Peak National Observatory, National Optical Astronomy Observatories, operated by the Association of Universities for Research in Astronomy, Inc., under contract with the National Science Foundation.
[2] Carnegie Fellow, 1983–1985.
[3] Now at the Space Telescope Science Institute, Baltimore, Maryland.
[4] Now at the University of Wisconsin.
[5] Operated by the Association of Universities for Research in Astronomy, Inc., for the National Aeronautics and Space Administration.

dynamics on the galactic scale. Each galaxy simply acts as a test body in the gravitational field of the other, without the complex interference of many near neighbors, as would be the case in a group or cluster environment. Interacting pairs can be simulated realistically with reasonably simple numerical models (e.g., van der Hulst 1978; Jenkins 1984). Comparisons between the results of those models and the data from observed binaries can provide considerable information about the evolution of pairs of galaxies. One particular numerical model and some preliminary results derived from its use are described in detail in Paper I (also Borne 1979, 1982). It was shown there that the uncomfortably short merger times (e.g., 10^9 yr) found by other investigators are probably correct to within a factor of 2. This time scale has suggested to White and Sharp (1977) and to Toomre (1977) that many pairs in the observed sample of double galaxies will merge in the next aeon and that a considerable number of pairs have merged in the past. In order to test this tidal friction hypothesis as well as to test further the validity of current gravitational interaction models, detailed analyses of individual binaries are needed. Such analyses require the selection of specific values for the various parameters that define each binary within the context of the particular physical model employed. The necessary observations and model results are now being collected for a sample of interacting pairs of galaxies. This paper describes the observational results for two specific interacting binaries, while a companion paper (Borne 1988*b*, hereafter Paper IV) presents numerical models that match these data. Future papers will report the results for several other pairs (Borne and Hoessel 1984; Borne, Balcells, and Hoessel 1988, hereafter Paper V). Using a numerical simulation algorithm as an interpretive tool, we elucidate in this series of papers the details of the galaxy interaction (and possible merger) process, and we identify what effects these interactions have on the internal workings of the galaxies themselves. A companion paper (Borne 1988*a*, hereafter Paper II) describes the simulation algorithm and the model-matching procedures in detail, and it argues the case for the uniqueness of the dynamical solutions.

Information pertaining to data acquisition and reduction procedures can be found in § II. Section III presents the observations (both spectroscopic and photometric) for two elliptical-elliptical pairs, K99 (NGC 1587/1588) and K564 (NGC 7236/7237). These are the data that are to be compared with various numerical simulations in Paper IV, where complete details of the best-fit models for these two binaries are presented. Section III also discusses what we believe to be observational signatures of tidal friction in action. Section IV concludes with discussions of (i) the importance of velocity measurements to studies of interacting binaries, and (ii) some interesting properties of NGC 1587.

II. OBSERVATIONS AND REDUCTIONS

a) Spectroscopy

Long-slit digital spectra have been obtained for several pairs of elliptical galaxies using the high-gain video spectrometer (HGVS) on the KPNO 4 m telescope. This instrument has been described by Kormendy and Illingworth (1982). The silicon intensifier target (hereafter SIT) Vidicon detector is read out in a 128 × 512 pixel configuration, with the long dimension parallel to the dispersion. The data discussed here were generally obtained by placing the length of the slit along the line connecting the centers of the two galaxies. Individual exposures were typically 50 minutes in duration, preceded and followed by exposures of the He-Ne-Ar comparison lamp. Dark frames of the SIT (i.e., with the transfer lens between the Vidicon tube and the three-stage image tube closed) were obtained every 2–3 hr. Exposures of the dark image tube, with the transfer lens open, were made at the beginning and end of each night, as were long exposures of the quartz flat-field calibration source. In addition, once per night, blank sky was observed for several minutes. The latter exposure was used to determine the large-scale slit response function.

All galaxies were observed at a single fixed grating setting that covered the wavelength range 3875–4590 Å. Each of the objects was selected on the basis of photometric evidence for interaction. Nearly all elliptical-elliptical pairs in the catalog of Karachentsev (1972) were observed with the SIT Vidicon area detector on the Palomar 1.5 m telescope (Borne, unpublished). Only those that had some sign of interaction (e.g., an asymmetric light distribution) were observed with the HGVS. All of these were sufficiently small in angular extent that both galaxies could be observed simultaneously with one telescope setting, while some blank sky was exposed concurrently at the ends of the slit. The latter was used for sky subtraction. Each pixel perpendicular to the dispersion corresponded approximately to 1".7. The slit width was 2", and the FWHM of a line in the comparison arc spectrum was ~4 pixels, or 3 times the projected slit width.

Reductions have been carried out with both the batch processing facilities and the IPPS system at KPNO using standard software packages. Standard processing begins with the subtraction of the bias level and the dark counts from each frame, followed by calibrations for both the individual pixel responses and for the large-scale slit response (i.e., the frames were "flattened"). The comparison lamp spectrum taken immediately before an object exposure is then used to map out and subsequently remove the pincushion distortion from the object exposure. It is at this point that the wavelength scale is set, which is followed by the rebinning of the data into equal increments of log λ, with the bin width equal to 99.15 km s^{-1}. The worst residuals for the dispersion/curvature fit were of order 30 km s^{-1} for any given spectral comparison line. Typical residuals were 10–20 km s^{-1}, scattered randomly about the best-fit polynomial. The S-distortion is then removed by (i) determining the position of the object (or the brightest portion of the object) perpendicular to the dispersion as a function of position along the dispersion, (ii) fitting a cubic polynomial to these points, and (iii) rewriting the entire data frame with the appropriate shifts perpendicular to the dispersion. Finally, for each data frame, the rows of blank sky at the ends of the slit are identified and added together in a 1 × 512 array, which is then subtracted row by row from the entire 128 × 512 data frame. Any repeat exposures of a particular object are then summed. Sums are made at this step, after the reductions are completed, in order to minimize any frame-to-frame spatial or wavelength drifts.

On late-type giant star (in the range from G8 III to K3 III) was observed each night. These were used as templates in the Fourier quotient program (hereafter FQP). That program determines radial velocity and velocity dispersion variations along the slit for each observed galaxy (Sargent *et al.* 1977). The stars were observed through a 2.5 mag neutral density filter and were trailed rapidly up and down the slit. This was done to prevent heavy charge buildup at any one location on the SIT, thus avoiding the complications of beam pulling

within the Vidicon (Schechter and Gunn 1979). Comparison arcs were likewise exposed through heavy neutral densities. The reduction of the standard star observations was handled in the same manner as the galaxy observations, except that there were no corrections for S-distortion (since stars are not extended objects), and no sky subtraction was necessary. For use by the FQP, each star frame was contracted to a 1 × 512 format, the result of which was a very high signal-to-noise standard star spectrum. In § III*a*, we discuss how our velocities depend on which particular template star is used in the analysis. For the purpose of improving the S/N in our object frames, adjacent rows in the extended spectrum of a galaxy were summed in groups of two or three.

The analysis of the prepared galaxy and star frames was handled by the FQP implemented at KPNO by D. McElroy, who followed the procedure developed by Sargent *et al.* (1977). One major additional step in the analysis of each data frame was to ignore the Ca II H and K region of each spectrum. It has been suggested that those heavily saturated lines can adversely affect velocity dispersion determinations (Schechter and Gunn 1979; Kormendy and Illingworth 1982). After a little experimentation, it appeared to us that there was no significant dependence of our measured velocities on the presence or absence of Ca II H and K in the digital spectra. Nevertheless, the collective experience of previous investigators has deemed it wise to excise that region of the spectral scans prior to running them through the FQP (Schechter and Gunn 1979; Kormendy and Illingworth 1982); this advice was followed. All of the rotation and dispersion profiles described in this paper were computed without H and K. The conventional wisdom states that the widths of these lines do not solely measure the velocity dispersion among the stars that contribute to the integrated galaxy spectrum, but the widths also measure the saturation within the lines themselves. It is also true that these lines are located in a region where there is a strong gradient in the continuum intensity, a gradient that is not perfectly matched between the galaxy and template star spectra. The effective wavelengths of H and K therefore do not accurately measure the recession velocity of the galaxy. Given the standard wisdom, the dominance of H and K in the given spectral range, and our interest in the specific variations of the rotation and dispersion velocities across each galaxy, we decided to ignore the spectral data around H and K.

b) Imaging

CCD pictures have been obtained for the same interacting galaxies for which HGVS observations exist. These data were collected at the KPNO 2.1 m telescope by G. E. Danielson and one of us (J. G. H.) using the Space Telescope wide-field planetary camera ground-based system, which consisted of an 800 × 800-pixel Texas Instruments CCD with a special optical couple that yields 0.″49 per pixel (Hoessel and Danielson 1983). Each exposure was made in the *r* (6500 Å) passband of Thuan and Gunn (1976); see Schneider, Gunn, and Hoessel (1983*a*) for a complete description of the photometric system. Typically, there were two exposures per object: a short exposure (1–2 minutes) for the study of the central regions of the galaxies, and a longer exposure (8–10 minutes) to bring up the low surface brightness features in the outermost parts of the light distribution.

Observations through a single filter are not sufficient to obtain absolute photometry. For that, a program to obtain quantitative surface photometry of a large sample of interacting galaxies is in progress and will be the subject of future contributions. Our immediate interest is in the relative photometric variations across the images of the galaxies as tracers of the tidal potential. For this, the present imaging data are sufficient.

Each exposure was reduced in the standard fashion: the bias level (i.e., "erase" frame) was subtracted from each of the pictures, each of which was then divided by the averaged flat field exposure for the night, followed by the subtraction of the mean sky level on the given frame. The photographs shown in this paper were obtained from the CCD frames with the KPNO IPPS and Dicomed facilities, and the contour plots were produced with a contouring program provided by D. P. Schneider (then at Caltech).

c) Summary of Observations

Two Karachentsev pairs are the subject of this first in a series of papers. These two are K99 and K564. Other names for K99 are NGC 1587/1588, II Zw 12, and Ho 76. The fainter of the two (NGC 1588) is Mk 616. Other names for K564 are NGC 7236/7237, Arp 169, II Zw 172, and 3C 442. A third component of Arp 169 is believed to be the projection of a galaxy at a different distance ($\Delta v = 700$ km s^{-1}; see § III*b* and Table 2).

HGVS observations of K99 and K564 in 1981 November spanned nearly 4 hr and 3 hr, respectively. CCD observations of K99 were 30, 120, and 600 s in duration, while for K564 they were 120 and 60 s. The CCD images were acquired in 1981 October in 1″–2″ seeing.

III. RESULTS FROM THE DATA ANALYSIS

a) K99 (NGC 1587/1588)

The photograph shown in Figure 1 (Plate 2) was made from the 600 s CCD exposure of K99; the print measures 4.′2 on a side. The larger galaxy is labeled "1" in this paper, with galaxy "2" located at separation 59″ and position angle 79° (measured east of north).

Contours of constant surface brightness are shown for K99 in Figure 2, where the levels are separated by a constant 0.75*r* mag arcsec^{-2}, with the highest level at 17.25*r* mag arcsec^{-2}. Calibration of the contours was made possible by a separate set of photometric images to be described in a later paper. Both Figures 1 and 2 have east and west reversed with respect to the appearance on the sky. The contours depicted in Figure 2 resulted from a combination of the two longest CCD exposures for K99. The 120 s exposure was used to locate the five innermost contour levels, while the five outermost levels were derived from the 600 s exposure.

From both Figures 1 and 2 one can recognize that K99-2 has a tail trailing to the south. This can also be seen on the Palomar Sky Survey print. What is now easy to see from Figure 2 is the asymmetric light distribution around K99-1. This galaxy is noticeably distended to the north. This pattern and that for K99-2 are suggestive not only of the presumed tidal interaction but also of motion in opposite directions for the two galaxies. It was this set of distortions in the light distribution that led us to select K99 for detailed observation. Of course, all of the pairs that were selected for study with the HGVS display some peculiarities in their photometric appearance. As described in Paper IV, the suggestions of motion and tidal interaction in K99 are supported by the results from a large number of simulations of this binary.

PLATE 2

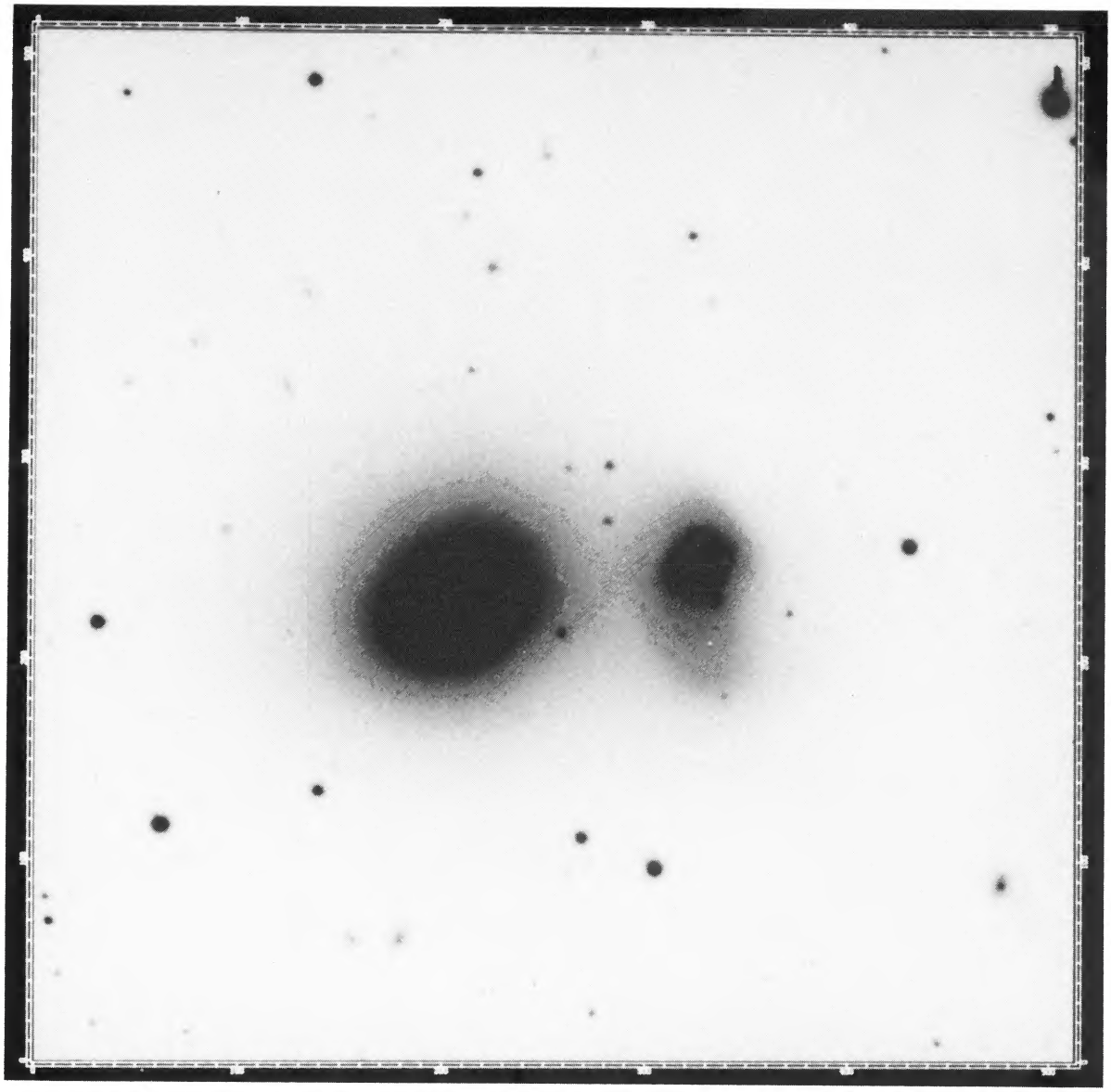

FIG. 1.—Ten minute red (6500 Å) CCD photograph of K99 from the KPNO 2.1 m, taken with the Wide Field/Planetary Camera ground-based system. North is up; east is to the right (reversed from the sky). Photo measures 4.2 on a side. Note the "tail" on the smaller galaxy.

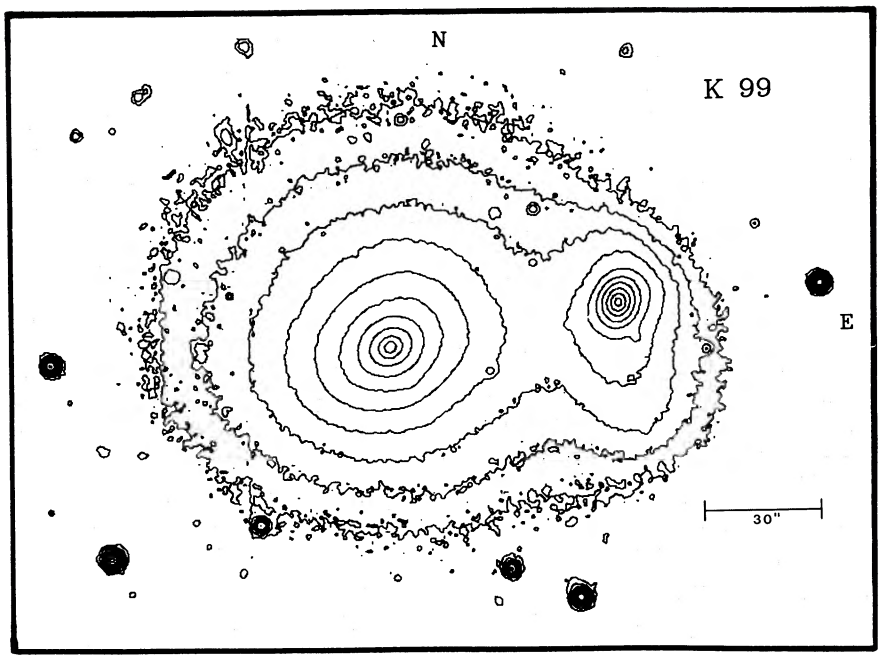

FIG. 2.—Contour plot for K99 derived from a combination of the CCD picture depicted in Fig. 1 and a 2 minute CCD exposure. North and east are as marked. The horizontal bar measures 30″. Contours represent constant red surface brightness, range from 17.25 to 24.0r mag arcsec^{-2}, and are separated by 0.75r mag arcsec^{-2}. The five innermost levels are derived from a short exposure, the five outermost levels from a long exposure. Of interest are the opposing distentions in the light distributions for the two galaxies.

Figure 3 (Plate 3) displays the fully processed two-dimensional K99 spectrum. Table 1 presents the central values of the redshift and velocity dispersion, and the uncertainties in these values, for the two components of K99, as determined by the FQP. These are tabulated for each template star observed during that run. The redshifts determined with star 3 seem spurious, presumably due to the mismatch between an elliptical galaxy spectrum and a G8 stellar spectrum. Such a mismatch can adversely affect the estimation of velocities from the Fourier quotient. It was decided then to run all of our remaining galaxy spectra through the FQP with a single star; HD 79214 (star 1) was chosen due to its steady behavior in the FQP. All velocities in Table 2 were determined using this star as the template. In that table, values for V_{corr} refer to recession velocities corrected for the motion of the Sun relative to the centroid of the Local Group.

The uncertainties quoted in Tables 1 and 2 are the errors estimated by the FQP in its determination of the width and phase shift of the velocity broadening function. Tabulated redshifts are actually weighted means of the values for the velocity shift measured at the three or four slit positions nearest the galaxy center. The value computed at a particular radius by the FQP was weighted by the inverse square of the error in the redshift determination at that radius. Such a weight is basically proportional to the total number of photons in the spectral scan at that position. Consequently, it was possible to assign both a realistic bulk velocity and a photon-weighted center to each galaxy on the HGVS scans.

Many other authors have reported velocities for one or both components of K99. For NGC 1587 (i.e., K99-1), we measure a corrected recession velocity of 3664 ± 10 km s^{-1}. Humason, Mayall, and Sandage (1965) measured 3826 ± 75 km s^{-1}; Lauque (1973) reported a value attributed to Zwicky also equal to 3826 km s^{-1}; Stocke, Tifft, and Kaftan-Kassim (1978) found 3275 ± 200 km s^{-1}; Karachentsev (1980) measured 3800 ± 50 km s^{-1}; Gallagher, Knapp, and Faber (1981) determined a bulk H I velocity for the whole K99 system equal to 3626 ± 11 km s^{-1}; and Tifft (1982) found 3522 ± 65 km s^{-1}. Tonry and Davis (1981) measured 3603 ± 22 km s^{-1} for the recessional velocity and 233 ± 27 km s^{-1} for the central velocity dispersion. Our redshift is roughly within 2 σ of most of these measurements and approximately equals the mean of all those values. For NGC 1588 (i.e., K99-2), we measure a corrected recession velocity of 3464 ± 8 km s^{-1}. Sargent (1970)

TABLE 1

FOURIER-QUOTIENT VELOCITIES FOR THE K99 PAIR

Star	Name	Type	$c(z_1 - z_0)$[a]	σ_1	$c(z_2 - z_0)$[b]	σ_2
1....	HD 79214	K0 III	106 ± 10	206 ± 11	-94 ± 8	138 ± 10
2....	HD 83820	K1 III	116 ± 11	216 ± 13	-103 ± 8	146 ± 11
3....	HD 214202	G8 III	52 ± 11	226 ± 12	-166 ± 8	149 ± 10

[a] $cz_0 = 3621$ km s^{-1} for K99. Subscript 1 denotes the west component of K99 (i.e., NGC 1587).

[b] Subscript 2 denotes the east component of K99 (i.e., NGC 1588).

TABLE 2

ADOPTED VELOCITIES AND DISPERSIONS

Galaxy	$c(z - z_0)$[a]	V_{corr}[b]	σ
K99-1 (west; NGC 1587)	106 ± 10	3664	206 ± 11
K99-2 (east; NGC 1588)	-94 ± 8	3464	138 ± 10
K564-1 (SE; NGC 7237)	-137 ± 11	8182	177 ± 14
K564-2 (NW; NGC 7236)	-164 ± 12	8155	183 ± 15
K564-3 (faint; SE)	-864 ± 32	7455	225 ± 42

[a] $cz_0 = 3621$ km s^{-1} for K99 and $cz_0 = 8106$ km s^{-1} for K564.

[b] Velocity corrected to centroid of the Local Group. This includes both the heliocentric correction and the standard solar motion correction: $\Delta v = 300 \sin l^{II} \cos b^{II}$.

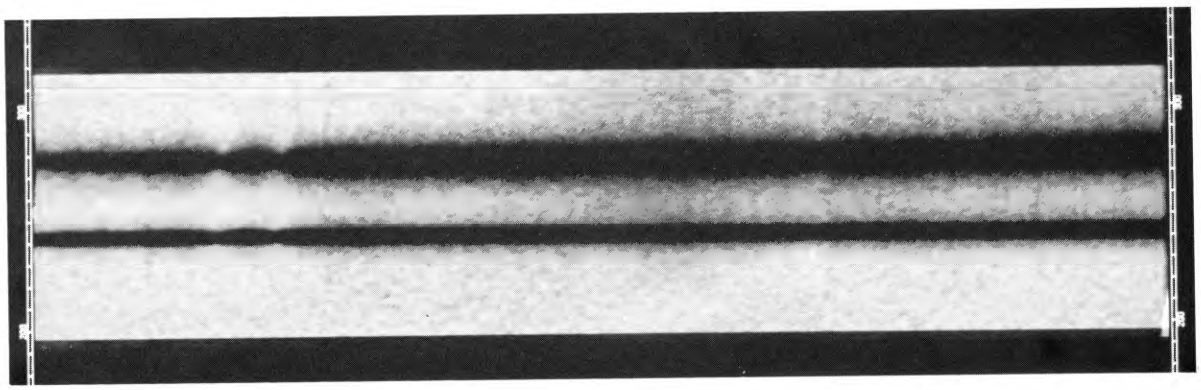

FIG. 3.—Print of the rectified two-dimensional long-slit spectrum of K99. Wavelength increases from left to right. Lower spectrum is that of the east component.

BORNE AND HOESSEL (*see* **330**, 54)

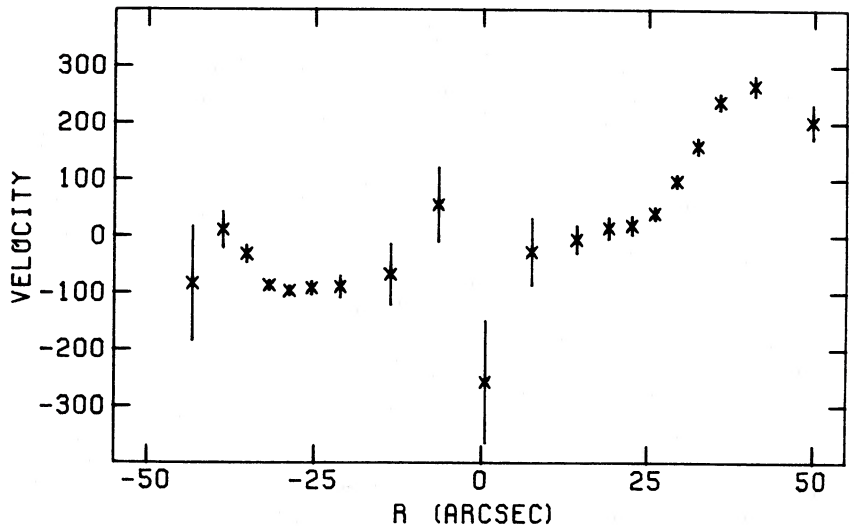

FIG. 4.—K99 rotation curve, along the line connecting the two galaxies. Velocity units are km s^{-1}, measured relative to $cz_0 = 3621$ km s^{-1}. East is to the left. The center of the east component is located at $R \approx -27''$ and that of the west component at $R \approx 32''$. The west component reveals an unusually large rotation rate for a galaxy of its type (E2). Of interest also is the peculiar U-shaped rotation profile for the east component (see text for a full discussion).

measured 3265 ± 60 km s^{-1}; Lauque (1973) reported a value attributed to Zwicky equal to 2966 km s^{-1}; Stocke, Tifft, and Kaftan-Kassim (1978) found 3812 ± 200 km s^{-1}; Karachentsev (1980) measured 3495 ± 90 km s^{-1}; and Tifft (1982) found 3452 ± 65 km s^{-1}. None of these low-weight measurements cast doubts on our FQP redshift.

Figures 4 and 5 show the radial variations of mean line-of-sight velocity and velocity dispersion, respectively, as extracted by the FQP from the reduced HGVS data for K99. The velocity units are km s^{-1}; R increases to the west (to the left in Figs. 1 and 2). The center of K99-1 is estimated to be located at $R \approx 32''$, with the center of K99-2 at $R \approx -27''$. As alluded to in the previous paragraph, these estimates are determined from a weighted mean of the locations of the points with the smallest errors in their velocity determination. The true relative velocity between the centers of the two galaxies is $\Delta v_{\rm true} = \Delta v_{\rm obs}/(1 + z) = 198 \pm 13$ km s^{-1}. Velocities in Figure 4 are measured relative to $cz_0 = 3621$ km s^{-1} (see Table 2). (This odd value for cz_0 owes to a zero-point correction to the redshifts that were originally calculated by the FQP; see Tonry 1985*b*.) K99-1 has a velocity range near 250 km s^{-1}, which is uncharacteristically large for an elliptical galaxy (Schechter and Gunn 1979). Similarly, its value of $v_{\rm rot}/\sigma_0 \approx 0.6$ is beyond the expected range for an E2 galaxy (Illingworth 1981). Unless K99-2 is unusually massive for its luminosity, with $(M/L)_2 \approx 10(M/L)_1$, and has a peculiarly low velocity dispersion for its mass, it is unlikely to have had much influence on the rotation properties of K99-1, especially in the inner 15″–20″ where the rotation profile is steep. The simulations presented in Paper IV for K99 assume an initial rotation velocity in galaxy 1 consistent with these observations since there was no success in the attempt to generate this degree of rotation through the application of tidal torques from galaxy 2. It is of interest to recall from the specific example of an interacting pair presented in Paper I that a rotation curve similar to that seen in K99-1 is not unusual for the remnant galaxy of a previous merger event.

K99-2 has no rotation near its center, but there is the suggestion in Figure 4 that its outer regions are moving away from the observer relative to the motion of its center. This apparent recession is seen on both sides of the galaxy, which is an impossible dynamical configuration for an isolated, undisturbed galaxy. Yet such a U-shaped velocity profile is not unusual for interacting galaxies. Of the nine Karachentsev pairs that we observed with the HGVS, the following have at least one galaxy with a U-shaped rotation curve: K99, K107, K340, and K564 (see Fig. 9). It is less clear for the other pairs, but the following also appear to have at least one galaxy with U-shaped "rotation": K143, K175, K194, and K204. These are

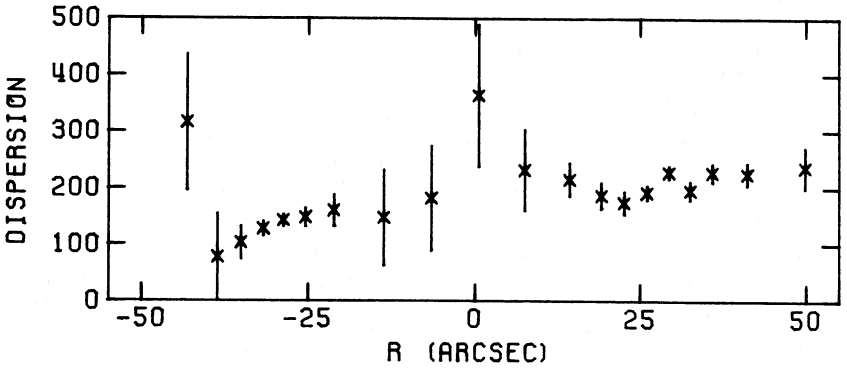

FIG. 5.—Spatial variations in the line-of-sight velocity dispersion for K99. Radial positions are the same as for the points shown in Fig. 4. Velocity units are km s^{-1}. East is to the left. Of interest is the positive gradient in the dispersion values for the east component.

uncertain because of the diminished S/N in their spectra at the radii of interest. Only K594 clearly lacks such a rotation curve; from the small rotation velocities and the small relative velocity of its component galaxies (no more than 100 km s^{-1}), we are apparently looking at K594 from an angle close to its orbital and rotation axes and we therefore do not expect any peculiarities in the shape of its line-of-sight velocity field. K594 and the other six Karachentsev pairs mentioned above will be discussed in more detail in later papers. In most of the cases where the U-shape is detectable, we are convinced that it is not a superposition effect. Between the two galaxies, at galactic radii beyond those where the upturn in the rotation is seen, we see a clear drop in the light detected by the spectrograph. There is simply not enough light contamination from the companion at radii corresponding to the rising sides of the U-curve to affect the integrated line-of-sight rotation profile.

Given the weight of evidence, it is nearly certain that a U-shaped rotation velocity curve is a signature of the tidal interaction in close pairs of galaxies (Borne and Hoessel 1985). How is such a velocity field possible? What prevents the stars from wrapping around the galaxy so that their individual velocity components add destructively on both sides of the galaxy, thereby erasing this remarkable rotation profile? Why do we see so many interacting pairs with at least one galaxy at this point in its dynamical evolution? The phenomenon either must be long-lived relative to the crossing time in a typical galaxy ($\sim 10^8$ yr), or else it must be directly related to the luminosity asymmetries that attracted our attention to these particular pairs of galaxies in the first place. Otherwise, why are so many of our observed distorted pairs found in this dynamical state? We believe in fact that these peculiar velocities are not long-lived, but are directly related to the luminosity distortions: both sets of observations provide visual evidence for tidal stripping and, consequently, tidal friction in action.

In order to best answer the questions posed in the previous paragraph, we draw attention to an unusual nonsymmetric tidal effect in a disturbed stellar system. As the center of mass responds to the bulk gravitational field of the disturbing object, the outermost stars are influenced relative to that center of mass by the differential (i.e., tidal) gravitational field. Stars moving retrograde with respect to the binary orbital motion are out of phase with the perturbation and tend to remain bound to their galaxy, while those moving prograde have a resonant response to the perturbation and have a greater probability of being stripped from their parent (e.g., Keenan and Innanen 1975; Jefferys 1976; Innanen 1979). In the present case, the prograde stars of each galaxy are being accelerated as a result of the gravitational interaction with the other galaxy and are being stripped, if not "boiled," out of their parent galaxy. Considering the low rotation velocity of most ellipticals (Illingworth 1981), such galaxies are composed of roughly equal numbers of stars populating the retrograde and prograde orbits. Among the prograde stars, those that are initially moving away from the perturber will be strongly braked (due to its in-phase response) and hence the net rotation of all stars, prograde and retrograde, on that side of the galaxy will be retrograde. The set of prograde stars that are initially moving toward the perturber will be strongly accelerated, leading to a net prograde rotation on that side of the galaxy. Therefore, opposing sides of the same galaxy can have net rotations in opposite directions, the result of which is a U-shaped rotation profile in which the outermost points on both sides of the galaxy are displaced in the same sense relative to the velocity at the center of the galaxy. This process looks very much like ablation. Given that their net motion is displaced with repect to the motion of the system center of mass, the most perturbed of these prograde stars can become separated (i.e., tidally stripped) from the galaxy center both in position and in velocity. We already anticipated this result from the observed luminosity asymmetries. Because the strength of the tidal field is of the same order as the internal gravitational field in those outer regions, the dynamical time scale for the tidal stripping is of the same order as the stellar crossing time within the galaxy. What occurs then is a violent, nonadiabatic process that does not allow the motions of the stars in the outermost parts of each galaxy to settle into a regular pattern for which each orbit, whether prograde or retrograde, is populated uniformly around the galaxy. It is therefore perfectly reasonable to expect that pairs that are selected for observation because of distortions in their light distribution will also demonstrate unusual, probably U-shaped, distortions in their rotation profiles.

To support further the interaction interpretation for these unusual rotation curves, many of the numerical simulations reported in Paper IV for both K99 and K564 were found to possess such rotation profiles. That the physical model described in Paper II can reproduce these observed curves assures us that the underlying physical phenomenon is of an ordinary gravitational nature. Because our gravitational encounter models end in merger through the action of tidal friction, we must conclude that *the U-shaped profiles and the asymmetric light distributions seen in these galaxies are evidence of tidal friction in action.* How these features signal tidal friction will be argued below (§ IV) and in greater detail in a forthcoming paper (see Borne and Hoessel 1985).

Figure 5 shows the variations in velocity dispersion across K99. As one would probably expect, given its larger size, K99-1 has higher values for the dispersion than does K99-2. The dispersion profile for K99-1 is relatively flat, with perhaps a slight increase toward galaxy 2. Dispersion values for K99-2 certainly increase from left to right on the plot, "heating up" toward K99-1. The latter pattern is perhaps another signature of the interaction, one that is less dependent than the rotation curve on the particular spatial orientations of the binary orbital and internal rotation vectors. Unfortunately, a positive dispersion gradient is at best a weak indicator of interaction if our sample of strongly distorted pairs are at all representative of the whole population of interacting binaries. Out of the nine observed Karachentsev pairs, only K99, K340, and K564 (see Fig. 10) present a nonzero gradient in the dispersion profile of at least one of their component galaxies.

b) K564 (NGC 7236/7237, 3C 442, Arp 169)

The photograph in Figure 6 (Plate 4) was made from the 600 s CCD picture of K564; the print measures 4.2 on a side. This picture is east-west reversed, as were Figures 1 and 2. The large galaxy to the southeast is labeled "1" in this paper. This galaxy is separated from galaxy "2" (to the northwest) by 34″ and is at position angle 126° relative to "2". The smaller galaxy to the southeast of the pair is labeled K564-3.

East and west are again reversed in Figure 7, which is the contour diagram generated from the CCD picture depicted in Figure 6. The contour level separation is a constant 0.75*r* mag $arcsec^{-2}$, with the highest level at 18.25*r* mag $arcsec^{-2}$ (calibrated by a separate set of photometric images to be

PLATE 4

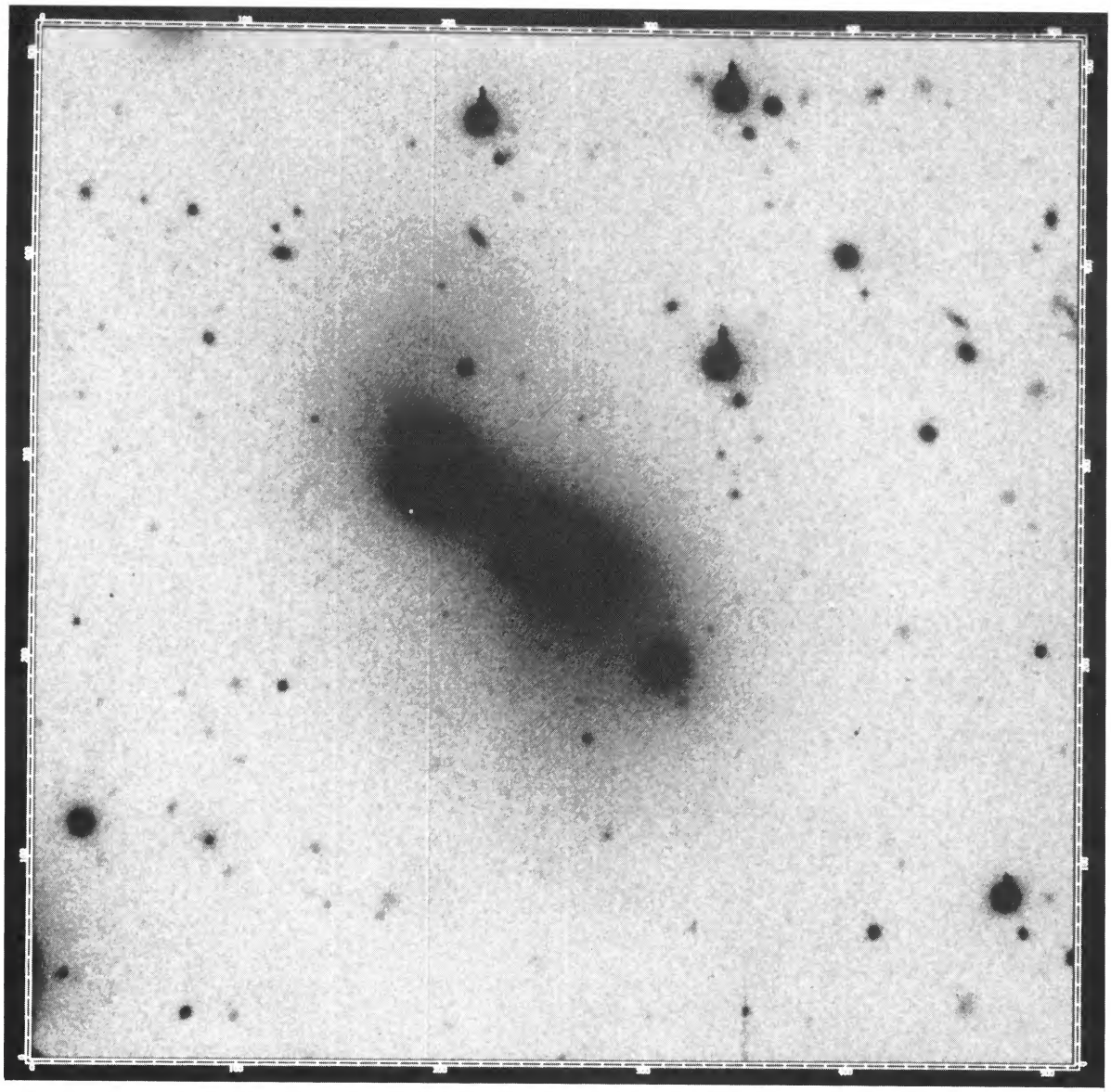

FIG. 6.—Ten minute red CCD photograph of K564 from the KPNO 2.1 m. North is up; east is to the right (reversed from sky). Photo measures 4'.2 on a side. Small component to the southeast is probably not closely associated with the larger interacting pair (see text for discussion).

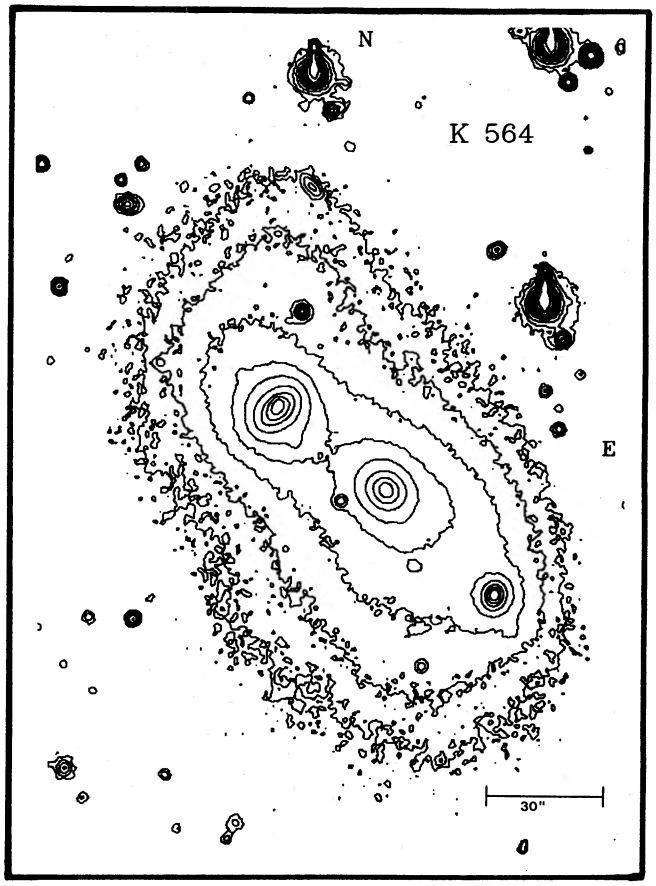

FIG. 7.—Contour plot for K564 derived from the CCD picture depicted in Fig. 6. North and east are as marked. The horizontal bar measures 30″. Contours represent constant red surface brightness, range from 18.25 to 24.25r mag arcsec^{-2}, and are separated by 0.75r mag arcsec^{-2}. Of interest are the sweeping distentions on opposing sides of the two main galaxies.

described in a later paper). Nine levels encompass the center of K564-2, while there is one less level at the centers of both K564-1 and −3.

A suggestive pattern appears in the photometric distortions of K564. As shown in Figure 7, each of the two main galaxies are more distended on one side than the other. These distentions are opposed for the two galaxies. Distended isophotes of this type were also seen in Figure 2 for K99, suggesting motion in the opposite direction, toward which the isophotes are seen to be more closely spaced. The simulations described in Paper IV indeed reproduce these isophotal patterns whenever the motions of the component galaxies are away from their distended sides. Finally, Figure 7 reveals a high degree of twisting in the isophotes for K564-2. These twists give evidence that the northwest component of K564, NGC 7236, is likely to be a strongly rotating S0 galaxy, not an elliptical, since stars in a rotating galaxy strongly couple to the tidal field of a perturber (see below and, e.g., Toomre and Toomre 1972). The best matching models presented in Paper IV are indeed those in which the simulated K564-2 has a strong rotation. Very slight evidence for a tail is seen in Figure 7 at position angle 305° (measured from north through east) on the fourth contour (counting from the outside). This "tail" was also detected and reported by Hayes and Comins (1984).

Figure 8 (Plate 5) displays the fully processed two-dimensional K564 spectrum. Table 2 presents the central values of the redshift (corrected to the centroid of the Local Group) and of the velocity dispersion for the three components of K564. The center of K564-3 was placed on the slit for a brief exposure following the extensive observations of K564 in which the slit was placed along the line connecting the two brightest components. It was found that the recession velocity measured for K564-3 differs from the values for the two main components by 700 km s^{-1}. Because of the magnitude of this difference and because of the bisymmetric pattern to the distortions in the light distribution around the two main galaxies, the third component of K564 likely has had no influence on the evolution of this binary and will henceforth be ignored throughout the remainder of this paper and Paper IV.

Many authors have reported velocities for the two brightest components of K564 (hereafter, just "the two components of K564"). For NGC 7236 (i.e., K564NW), we measured a corrected recessional velocity of 8155 ± 12 km s^{-1} (corrected to the centroid of the Local Group). Greenstein (1962) found 8097 ± 30 km s^{-1}, Jenner (1974) reported 8107 ± 72 km s^{-1}, and Tifft (1982) measured 8212 ± 65 km s^{-1}. Tonry and Davis (1981) measured 8116 ± 21 km s^{-1} for the recessional velocity and 257 ± 17 km s^{-1} for the central velocity dispersion. For NGC 7237 (i.e., K564SE), we measured 8182 ± 11 km s^{-1}. Greenstein (1962) reported 8092 ± 30 km s^{-1}, Jenner (1974) measured 8106 ± 72 km s^{-1}, and Tifft (1982) found 7964 ± 65 km s^{-1}. The recessional velocity and central dispersion presented by Tonry and Davis (1981) are 8074 ± 28 km s^{-1} and 225 ± 31 km s^{-1}, respectively. Our values agree well with most of these, except for the velocity dispersions.

The true relative velocity between the two components of K564 is 26 ± 16 km s^{-1}, which is just enough different from zero so as to be useful in matching models to the observations for this binary (see Paper IV). From their observations, Hayes and Comins (1984) report an upper limit to the velocity difference of 25 km s^{-1}, in agreement with our measurement. As seen in Table 2, there appears to be no significant difference in the central velocity dispersions for the two components. In fact, if the uncertainties were to be ignored, then K564-1, the larger galaxy and the one that has the lower central surface brightness, would have the smaller of the two central velocity dispersions. From these observations it is not clear which galaxy is the most massive. In Paper IV, we present simulations in which a mass ratio of unity is assumed. Such a value probably could be better tuned to the data, but how the mass is apportioned between the two model galaxies does not strongly affect the estimate given in that paper for the total mass of the binary. Even so, we expect the true mass ratio of the K564 pair to be within a few percent of unity.

Figures 9 and 10 depict the positional dependence of the mean line-of-sight velocity and velocity dispersion, respectively, as determined by the FQP from the reduced HGVS data for K564. As in Figures 4 and 5, the velocity units are km s^{-1}. Unlike Figures 4 and 5, distance R increases to the east for Figures 9 and 10. The rightmost data point in both Figures 9 and 10 is in the direction toward the center of K564-3. The centers of K564-1 and -2 are estimated to be located at $R \approx 17''$ and $R \approx -18''$, respectively.

The total range of velocities in Figure 9 for K564 is less than was seen in Figure 4 for K99. Velocities in Figure 9 are measured relative to $cz_0 = 8106$ km s^{-1} (see Table 2). (As mentioned above, this unusual value for cz_0 derives from a zeropoint correction to the originally calculated redshifts from

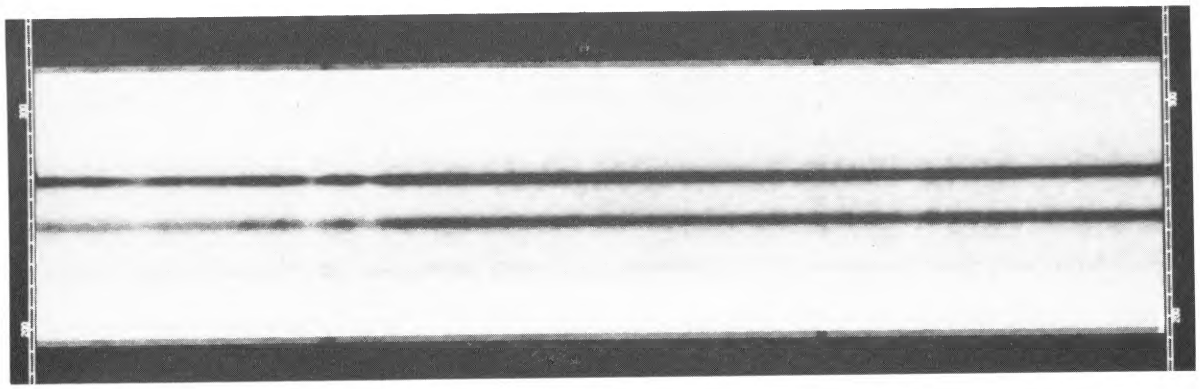

FIG. 8.—Print of the rectified two-dimensional long slit spectrum of K564. Wavelength increases from left to right. Upper spectrum is that of the NW component.

BORNE AND HOESSEL (*see* **330**, 57)

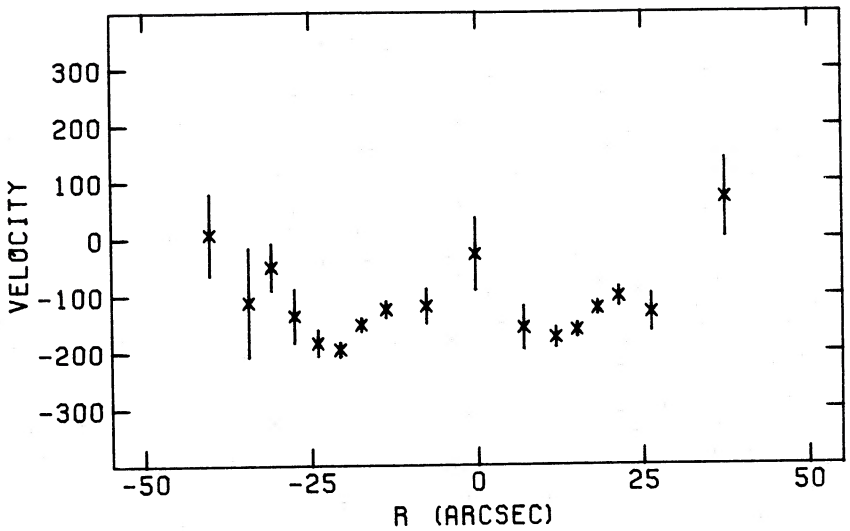

FIG. 9.—K564 rotation curve, along the line connecting the two galaxies. Velocity units are km s^{-1}, measured relative to $cz_0 = 8106$ km s^{-1}. East is to the right. The center of the west component is located at $R \approx -18''$ and that of the east component at $R \approx 17''$. Of interest is the unusual U-shaped rotation profile for the west component.

the FQP; see Tonry 1985*b*.) A positive rotation-velocity gradient is evident near the centers of both galaxies. However, the trend in the points to the left of the center of galaxy 2 corresponds to a negative gradient. Given the number of data points involved in the trend, this turnaround in the rotation curve is probably real. The corresponding U-shaped rotation profile that this suggests for K564-2 was alluded to earlier in the discussion of a similarly peculiar profile measured for K99-2. This pattern is again considered to be a signature of the interaction. The apparent lack of such a signature in the velocity profile for K564-1 may be due to its different dynamical orientation relative to the observer. Given that the flattening of K564-1 is along the slit, while that of K564-2 is orthogonal to the slit, the apparent disturbances in the velocity fields of the two galaxies need not be similar. We believe that the line-of-sight velocity field for K564-1 does in fact have an inverted U-shaped component and that it will be seen when higher S/N spectra of the outermost regions of this galaxy are obtained. In fact, the second rightmost point for K564-1 (not the point nearest to K564-3) is consistent with this suggestion. Most of the simulations described in Paper IV demonstrate the physical significance of these turnarounds in the rotation curves.

Figure 10 presents the velocity dispersion variations across K564. There may be a slight tendency in each galaxy for the dispersion values to increase toward the companion galaxy. This was alluded to in the discussion for K99-2, whose dispersion profile displays a significant gradient. Again, this may be due to increased tidal heating of the stars in the region between the two galaxies where the gravitational interaction is strongest. Of course, in the case of K564 where the overlap of the galaxy images is greater than in K99, the increased dispersion in the line-of-sight velocities between the galaxies may also derive partly from the superposition of the two kinematic components of the starlight (i.e., our line of sight intersects stars from both galaxies). For the most part, Figure 10 suggests that the line-of-sight velocity dispersion values have very little radial dependence.

IV. DISCUSSION

One of the most important results obtained from the observations reported here is the identification of signatures of tidal friction. Nearly all models of interacting galaxies predict that the orbit of the pair will decay and that the two will become one in a merger event. However, little observational evidence has been offered in support of the tidal friction (or merger) hypothesis. There has been no lack of data to support the

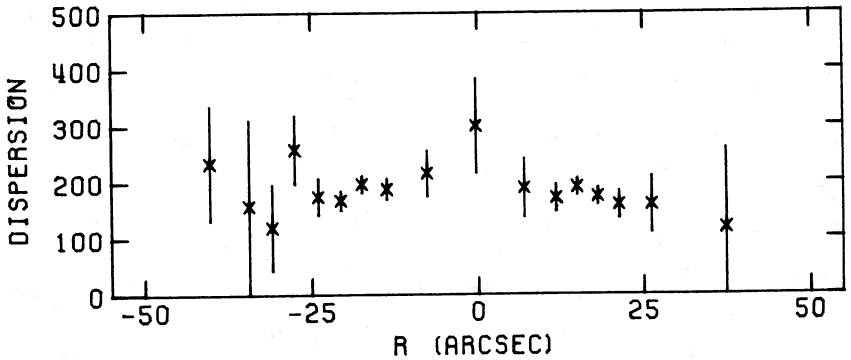

FIG. 10.—Spatial variations in the line-of-sight velocity dispersion for K564. Radial positions are the same as for the points shown in Fig. 9. Velocity units are km s^{-1}; east is to the right.

gravitational interaction hypothesis for the origin of unusual properties in galaxies, but that does not prove that galaxies in pairs will coalesce during an encounter. We believe that our observations uncover properties of interacting binaries that not only trace the orbital history, but also signal orbital decay. First, asymmetric light distributions in close pairs of galaxies prove to be indicators of the direction of motion of the galaxies: the distended bulge of stars *trails* the parent galaxy during a close encounter. Second, the rotation curves for many of the ellipticals in close pairs are U-shaped: opposite sides of a perturbed galaxy are each moving in the same absolute direction, opposite that of the galaxy's luminosity center. Stars in the photometric tail are related to those contributing to the wings of the U-shaped rotation profile in that both sets of stars are being extracted from the galaxy. A spin-orbit coupling is responsible for both effects: tidal stripping occurs preferentially among those stars moving prograde with respect to the perturbing galaxy. Angular momentum is transferred from the binary orbit to the motions of these stars. Such a transfer will lead to the predicted orbital decay and eventual merger of the pair.

Gallagher, Knapp, and Faber (1981) have emphasized the importance of velocity measures when studying interacting galaxies. From our discussion above and from the investigations reported in Paper IV we draw a similar but stronger conclusion: that the addition of velocity measures to detailed imaging data is required in order to fully determine the dynamical state of interacting and other disturbed galaxies (see Papers II and IV). A wide selection of simulations can be found that match only the morphological disturbances in a pair of galaxies. It is the long-slit velocity data that truly constrain the projection factors, mass estimates, and orbital configurations (see also Sharp 1986). In Paper IV, specific model simulations are presented for K99 and K564, from which mass estimates and three-dimensional orientations are derived for these two systems. That these solutions are unique is argued in general terms, but nevertheless in detail, in Paper II.

Because images of galaxies can be acquired through wide-band observations, imaging data are measurable to fainter limits (where tidal effects are most strongly evident) and are thus potentially of more value than the elusive narrow-band spectroscopic data measurable only at small radii. Yet because of the great importance of the velocity data, even if central redshifts and central dispersions alone were available (in addition to good surface photometry), then all would not be lost. On the contrary, it would still be possible to use most of the arguments that were laid out in Paper II to place physically significant constraints on the physical parameters of an interacting binary. In fact, such data are easily obtainable for a very large sample of interacting galaxy pairs. Ascertaining the dynamical status of a significant number of pairs is thus within reach. A data base of this type, consisting of both surface photometry and central velocity measures, is now being compiled. Later papers will present surface photometric measurements and dynamical data (i.e., central redshifts and dispersions) for many of the Karachentsev E-E pairs. Detailed analyses of several specific pairs are also forthcoming; through the application of the procedures described in Paper II, we can provide mass estimates and an appraisal of the dynamical state for each system. Papers IV and V present the first of these analyses. From the impending compilation of binary separations and M/L estimates, one can look for correlations between these two parameters and attempt to measure the extent of dark halos surrounding elliptical galaxies. At this point, using the results of Paper IV, we can only state that massive dark halos are not required to reproduce the observed photometric distortions and velocities in the two interacting pairs of ellipticals studied here. But then this is the expected conclusion since the binary separations in the K99 and K564 pairs are of order 10 kpc, a distance at which halos exert little tidal dynamical influence.

The binaries described in this paper obviously are not yet merged. Yet the rotation rate of the primary galaxy in K99, NGC 1587, is considerably more than that of the typical E2 galaxy. It was shown in Paper I that such high rotation rates can be produced in a merger episode. A specific example of a merged galaxy is presented in Paper I; it has properties very similar to NGC 1587. Perhaps this galaxy is a merger remnant about to "consume" yet another companion. In fact, Gallagher, Knapp, and Faber (1981) present H I radio measures for this system, suggesting an unusual origin for NGC 1587, which otherwise resembles a typical *elliptical* galaxy. Perhaps here is an elliptical galaxy that has not only formed through a merger event, but is still growing through the capture of additional satellite galaxies. Jenkins (1981) indeed suggests that some radio ellipticals are merger remnants, whereas Heckman (1983) would argue that enhanced radio emissions are stimulated by the current encounter. After studying this latter question in detail, Heckman *et al.* (1986) conclude that very powerful radio sources are associated with both colliding galaxies and merger remnants.

Whatever the origin of the rotation in NGC 1587, further spectroscopic observations of this galaxy would be of tremendous value. Measurements at various slit position angles will provide a detailed map of the velocity field in this galaxy and in its companion. Not only could we investigate the nature of the high rotation rate in NGC 1587, but we could also determine if indeed the dynamical simulations of Paper IV fully describe the dynamical state of the K99 binary system. The tidal interaction and merger hypotheses can then be rigorously tested against these more detailed spectroscopic data.

We would like to thank J. Westphal and J. Gunn for making available the equipment used for the imaging observations reported here, and Ed Danielson for help in obtaining them. Don Schneider provided image processing software and helpful discussions. We thank Doug McElroy for making available his FQP and for considerable assistance in its use. K. D. B. wishes to thank J. Gunn for additional advice and encouragement and to thank an anonymous referee for several useful suggestions. K. D. B. was supported in part by NSF grant 82-02930 to the University of Michigan, and in part by a Carnegie Fellowship at DTM.

REFERENCES

Borne, K. D. 1979, *Bull. AAS*, **11**, 673.
———. 1982, Ph.D. thesis, Caltech.
———. 1984, *Ap. J.*, **287**, 503 (Paper I).
———. 1988*a*, *Ap. J.*, **330**, 38 (Paper II).
———. 1988*b*, *Ap. J.*, **330**, 61 (Paper IV).
Borne, K. D., Balcells, M., and Hoessel, J. G. 1988, *Ap. J.*, submitted (Paper V).
Borne, K. D., and Hoessel, J. G. 1984, *Bull. AAS*, **16**, 881.
———. 1985, *Bull. AAS*, **17**, 601.
Borne, K. D., and Richstone, D. O. 1982, *Bull. AAS*, **14**, 972.
———. 1988, preprint.

Carter, D., Efstathiou, G., Ellis, R. S., Inglis, I., and Godwin, J. 1981, *M.N.R.A.S.*, **195**, 15p.
Cowie, L. L., and Hu, E. M. 1986, *Ap. J.* (*Letters*), **305**, L39.
Davies, R. L., Efstathiou, G., Fall, S. M., Illingworth, G., and Schechter, P. L. 1983, *Ap. J.*, **266**, 41.
Gallagher, J. S., Knapp, G. R., and Faber, S. M. 1981, *A.J.*, **86**, 1781.
Greenstein, J. L. 1962, *Ap. J.*, **135**, 679.
Hausman, M. A., and Ostriker, J. P. 1978, *Ap. J.*, **224**, 308.
Hayes, J. J. E., and Comins, N. F. 1984, *Bull. AAS*, **16**, 962.
Heckman, T. M. 1983, *Ap. J.*, **268**, 628.
Heckman, T. M., Smith, E. P., Baum, S. A., Breugel, W. J. M., Miley, G. K., Illingworth, G. D., Bothun, G. D., and Balick, B. 1986, *Ap. J.*, **311**, 526.
Hoessel, J. G., Borne, K. D., and Schneider, D. P. 1985, *Ap. J.*, **293**, 94.
Hoessel, J. G., and Danielson, G. E. 1983, *Pub. A.S.P.*, **95**, 336.
Hoessel, J. G., and Schneider, D. P. 1985, *A.J.*, **90**, 1648.
Humason, M. L., Mayall, N. U., and Sandage, A. R. 1956, *A.J.*, **61**, 97.
Illingworth, G. 1981, in *The Structure and Evolution of Normal Galaxies*, ed. S. M. Fall and D. Lynden-Bell (Cambridge: Cambridge University Press), p. 27.
———. 1983, in *IAU Symposium 100, Internal Kinematics and Dynamics of Galaxies*, ed. E. Athanassoula (Dordrecht: Reidel), p. 257.
Innanen, K. A. 1979, *A.J.*, **84**, 960.
Jefferys, W. H. 1976, *A.J.*, **81**, 983.
Jenkins, C. R. 1981, *M.N.R.A.S.*, **196**, 987.
———. 1984, *Ap. J.*, **277**, 501.
Jenner, D. C. 1974, *Ap. J.*, **191**, 55.
Karachentsev, I. D. 1972, *Comm. Spec. Ap. Obs. USSR*, **7**, 3.
———. 1980, *Ap. J. Suppl.*, **44**, 137.
Keenan, D. W., and Innanen, K. A. 1975, *A.J.*, **80**, 290.
Kormendy, J., and Illingworth, G. 1982, *Ap. J.*, **256**, 460.
Lauque, R. 1973, *Astr. Ap.*, **23**, 253.
Merritt, D. 1984, *Ap. J.* (*Letters*), **280**, L5.
Ostriker, J. P., and Tremaine, S. D. 1975, *Ap. J.* (*Letters*), **202**, L113.
Quinn, P. J. 1984, *Ap. J.*, **279**, 596.
Sargent, W. L. W. 1970, *Ap. J.*, **160**, 405.
Sargent, W. L. W., Schechter, P. L., Boksenberg, A., and Shortridge, K. 1977, *Ap. J.*, **212**, 326.
Schechter, P. L., and Gunn, J. E. 1979, *Ap. J.*, **229**, 472.
Schneider, D. P., and Gunn, J. E. 1982, *Ap. J.*, **263**, 14.
Schneider, D. P., Gunn, J. E., and Hoessel, J. G. 1983*a*, *Ap. J.*, **264**, 337.
———. 1983*b*, *Ap. J.*, **268**, 476.
Schweizer, F. 1982, *Ap. J.*, **252**, 455.
———. 1983, in *IAU Symposium 100, Internal Kinematics and Dynamics of Galaxies*, ed. E. Athanassoula (Dordrecht: Reidel), p. 319.
Schweizer, F., Whitmore, B. C., and Rubin, V. C. 1983, *A.J.*, **88**, 909.
Sharp, N. A. 1986, in *IAU Symposium 117, Dark Matter in the Universe*, ed. J. Kormendy and G. R. Knapp (Dordrecht: Reidel), p. 96.
Stocke, J. T., Tifft, W. G., and Kaftan-Kassim, M. A. 1978, *A.J.*, **83**, 322.
Thuan, T. X., and Gunn, J. E. 1976, *Pub. A.S.P.*, **88**, 543.
Tifft, W. G. 1982, *Ap. J. Suppl.*, **50**, 319.
Tonry, J. L. 1984, *Ap. J.*, **279**, 13.
———. 1985*a*, *Ap. J.*, **291**, 45.
———. 1985*b*, *A.J.*, **90**, 2431.
Tonry, J. L., and Davis, M. 1981, *Ap. J.*, **246**, 666.
Toomre, A. 1977, in *The Evolution of Galaxies and Stellar Populations*, ed. B. M. Tinsley and R. B. Larson (New Haven: Yale University Observatory), p. 401.
Toomre, A., and Toomre, J. 1972, *Ap. J.*, **178**, 623.
Tremaine, S. 1981, in *The Structure and Evolution of Normal Galaxies*, ed. S. M. Fall and D. Lynden-Bell (Cambridge: Cambridge University Press), p. 67.
van der Hulst, J. M. 1978, in *IAU Symposium 77, Structure and Properties of Nearby Galaxies*, ed. E. M. Berkhuijsen and R. Wielebinski (Dordrecht: Reidel), p. 269.
White, S. D. M. 1976, *M.N.R.A.S.*, **174**, 19.
White, S. D. M., and Rees, M. J. 1978, *M.N.R.A.S.*, **183**, 341.
White, S. D. M., and Sharp, N. A. 1977, *Nature*, **269**, 395.

KIRK D. BORNE: Space Telescope Science Institute, Homewood Campus, Baltimore, MD 21218

JOHN G. HOESSEL: Department of Astronomy, University of Wisconsin, 475 N. Charter St., Madison, WI 53706